Interlaced cholesteric liquid crystal fingerprint textures via sequential UV-induced polymer-stabilization

Wen-Song Li, [1] Ling-Ling Ma, [1, 2] Ling-Li Gong, [1] Sen-Sen Li, [1] Can Yang, [1] Bin Luo, [1] Wei Hu, [2] and Lu-Jian Chen[1, 3, *]

[1]*Department of Electronic Engineering, School of Information Science and Engineering, Xiamen University, Xiamen 361005, China*

[2]*National Laboratory of Solid State Microstructures, Collaborative Innovation Center of Advanced Microstructures and College of Engineering and Applied Sciences, Nanjing University, Nanjing 210093, China*

[3]*State Key Laboratory of Silicon Materials, Zhejiang University, Hangzhou, 310027, China*

[*]*lujianchen@xmu.edu.cn.*

Abstract: Two types of cholesteric liquid crystal (CLC) fingerprint structures, namely developable-modulation (DM) and growing-modulation (GM), can be contemporaneously prepared in polymer stabilized CLC (PSCLC) composites, to be mutually perpendicular in a repeatable and reversible voltage-switching process when the cell thickness to pitch length ratios (*d*/*P*) were appropriately chosen. PSCLC grating structures with interlaced DM/GM fingerprint textures were achieved by varying the applied voltage and sequentially photopolymerizing the dissolved mesogenic monomers through photomasks with stripe and checker patterns. The morphologies of the distinct interlaced PSCLC structures via different UV exposure sequences were investigated under crossed polarizing optical microscopy (POM) and scanning electron microscopy (SEM). The optimized results suggest that DM gratings should be stabilized before GM gratings. Diffraction measurements reveal polarization-dependent properties of the interlaced DM/GM gratings. The intensity redistribution of diffraction orders in orthogonal direction can be achieved by changing the polarization state of incident laser beam.

OCIS codes: (160.3710) Liquid crystals; (050.1950) Diffraction gratings.

References and links

1. V. I. Kopp, B. Fan, H. K. M. Vithana, and A. Z. Genack, "Low-threshold lasing at the edge of a photonic stop band in cholesteric liquid crystals," Opt. Lett. **23**(21), 1707–1709 (1998).
2. M. Mitov and N. Dessaud, "Going beyond the reflectance limit of cholesteric liquid crystals," Nat. Mater. **5**(5), 361–364 (2006).
3. A. Mujahid, H. Stathopulos, P. A. Lieberzeit, and F. L. Dickert, "Solvent vapour detection with cholesteric liquid crystals--optical and mass-sensitive evaluation of the sensor mechanism," Sensors (Basel) **10**(5), 4887–4897 (2010).
4. C. Y. Huang, K. Y. Fu, K. Y. Lo, and M. S. Tsai, "Bistable transflective cholesteric light shutters," Opt. Express **11**(6), 560–565 (2003).
5. D. Subacius, P. J. Bos, and O. D. Lavrentovich, "Switchable diffractive cholesteric gratings," Appl. Phys. Lett. **71**(10), 1350–1352 (1997).
6. O. D. Lavrentovich, S. V. Shiyanovskii, and D. Voloschenko, "Fast beam steering cholesteric diffractive devices," Proc. SPIE **3787**, 149–155 (1999).
7. A. Y.-G. Fuh, C. H. Lin, and C. Y. Huang, "Dynamic pattern formation and beam-steering characteristics of cholesteric gratings," Jpn. J. Appl. Phys. **41**(1), 211–218 (2002).
8. H. C. Jau, T. H. Lin, Y. Y. Chen, C. W. Chen, J. H. Liu, and A. Y.-G. Fuh, "Direction switching and beam steering of cholesteric liquid crystal gratings," Appl. Phys. Lett. **100**(13), 131909 (2012).
9. H. S. Jeong, Y. H. Kim, J. S. Lee, J. H. Kim, M. Srinivasarao, and H. T. Jung, "Chiral nematic fluids as masks for lithography," Adv. Mater. **24**(3), 381–384 (2012).

#253234 Received 4 Nov 2015; revised 30 Nov 2015; accepted 30 Nov 2015; published 3 Dec 2015

10. K. L. Lee, J. J. Wu, T. J. Chen, Y. S. Wu, F. C. Chen, and S. H. Chen, "Brightness enhancement with a fingerprint chiral nematic liquid crystal," Jpn. J. Appl. Phys. **50**(3R), 032601 (2011).
11. D. Subacius, S. V. Shiyanovskii, P. Bos, and O. D. Lavrentovich, "Cholesteric gratings with field-controlled period," Appl. Phys. Lett. **71**(23), 3323–3325 (1997).
12. J. J. Wu, Y. S. Wu, F. C. Chen, and S. H. Chen, "Formation of phase gratings in planar aligned cholesteric liquid crystal film," Jpn. J. Appl. Phys. **41**(2), L1318–L1320 (2002).
13. D. Voloschenko and O. D. Lavrentovich, "Light-induced director-controlled microassembly of dye molecules from a liquid crystal matrix," J. Appl. Phys. **86**(9), 4843–4846 (1999).
14. T. Ishikawa and O. D. Lavrentovich, *Defects in Liquid Crystals: Computer Simulations, Theory and Experiments* (Kluwer Academic Publishers, 2001), pp. 271–301.
15. W. Helfrich, "Electrohydrodynamic and dielectric instabilities of cholesteric liquid crystals," J. Chem. Phys. **55**(2), 839–842 (1971).
16. W. Helfrich, "Deformation of cholesteric liquid crystals with low threshold voltage," Appl. Phys. Lett. **17**(12), 531–532 (1970).
17. H. C. Jau, T. H. Lin, R. X. Fung, S. Y. Huang, J. H. Liu, and A. Y.-G. Fuh, "Optically-tunable beam steering grating based n azobenzene doped cholesteric liquid crystal," Opt. Express **18**(16), 17498–17503 (2010).
18. A. Ryabchun, A. Bobrovsky, J. Stumpe, and V. Shibaev, "Electroinduced diffraction grating in cholesteric polymer with phototunable helix pitch," Adv. Optical Mater. DOI: 10.1002/adom.201500293 (posted 14 July 2015, in press).
19. I. Gvozdovskyy, O. Yaroshchuk, and M. Serbina, "Light-induced nematic - cholesteric structural transitions in the LC cells with homeotropic anchoring," Mol. Cryst. Liq. Cryst. (Phila. Pa.) **546**, 202–208 (2011).
20. S. Kurihara, S. Nomiyama, and T. Nonaka, "Photochemical control of the macrostructure of cholesteric liquid crystals by means of photoisomerization of chiral azobenzene molecules," Chem. Mater. **13**(6), 1992–1997 (2001).
21. I. Gvozdovskyy, O. Yaroshchuk, M. Serbina, and R. Yamaguchi, "Photoinduced helical inversion in cholesteric liquid crystal cells with homeotropic anchoring," Opt. Express **20**(4), 3499–3508 (2012).
22. A. Ryabchun, A. Bobrovsky, J. Stumpe, and V. Shibaev, "Rotatable diffraction gratings based on cholesteric liquid crystals with phototunable helix pitch," Adv. Optical Mater. DOI: 10.1002/adom.201500159 (posted 6 May 2015, in press).
23. C. H. Lin, R. H. Chiang, S. H. Liu, C. T. Kuo, and C. Y. Huang, "Rotatable diffractive gratings based on hybrid-aligned cholesteric liquid crystals," Opt. Express **20**(24), 26837–26844 (2012).
24. L. L. Ma, S. S. Li, W. S. Li, W. Ji, B. Luo, Z. G. Zheng, Z. P. Cai, V. Chigrinov, Y. Q. Lu, W. Hu, and L. J. Chen, "Rationally designed dynamic superstructures enabled by photoaligning cholesteric liquid crystals," Adv. Optical Mater. DOI: 10.1002/adom.201500403 (posted 7 September 2015, in press).
25. S. N. Lee, L. C. Chien, and S. Sprunt, "Polymer-stabilized diffraction gratings from cholesteric liquid crystals," Appl. Phys. Lett. **72**(8), 885–887 (1998).
26. S. W. Kang, S. Sprunt, and L. C. Chien, "Structure and morphology of polymer-stabilized cholesteric diffraction gratings," Appl. Phys. Lett. **76**(24), 3516–3518 (2000).
27. S. W. Kang, S. Sprunt, and L. C. Chien, "Photoinduced localization of orientationally ordered networks at the surface of a liquid crystal host," Macromolecules **35**(25), 9372–9376 (2002).
28. H. C. Jau, Y. N. Li, C. C. Li, C. W. Chen, C. T. Wang, H. K. Bisoyi, T. H. Li, T. J. Bunning, and Q. Li, "Light-driven wide-range nonmechanical beam steering and spectrum scanning based on a self-organized liquid crystal grating enabled by a chiral molecular switch," Adv. Optical Mater. **3**(2), 166–170 (2015).
29. S. W. Kang, S. Sprunt, and L. C. Chien, "Polymer-stabilized cholesteric diffraction gratings-effects of UV wavelength on polymer morphology and electrooptic properties," Chem. Mater. **18**(18), 4436–4441 (2006).
30. A datasheet provided by Yantai Xianhua Chem-Tech Co, LTD, China.
31. I. A. Yao, Y. C. Lai, S. H. Chen, and J. J. Wu, "Relaxation of a field-unwound cholesteric liquid crystal," Phys. Rev. E Stat. Nonlin. Soft Matter Phys. **70**(5), 051705 (2004).
32. J. V. Gandhi, X. D. Mi, and D. K. Yang, "Effect of surface alignment layers on the configurational transitions in cholesteric liquid crystals," Phys. Rev. E Stat. Phys. Plasmas Fluids Relat. Interdiscip. Topics **57**(6), 6761–6766 (1998).
33. V. A. Belyakov, E. I. Kats, and S. P. Palto, "Temperature and field hysteresis of the pitch variations in thin planar layers of cholesterics," Mol. Cryst. Liq. Cryst. (Phila. Pa.) **410**(1), 229–238 (2004).
34. V. A. Belyakov, I. W. Stewart, and M. A. Osipov, "Surface anchoring and dynamics of jump-wise director reorientations in planar cholesteric layers," Phys. Rev. E Stat. Nonlin. Soft Matter Phys. **71**(5), 051708 (2005).
35. A. D. Kiselev and T. J. Sluckin, "Twist of cholesteric liquid crystal cells: Stability of helical structures and anchoring energy effects," Phys. Rev. E Stat. Nonlin. Soft Matter Phys. **71**(3), 031704 (2005).
36. I. Gvozdovskyy, "Influence of the anchoring energy on jumps of the period of stripes in thin planar cholesteric layers under the alternating electric field," Liq. Cryst. **41**(10), 1495–1504 (2014).
37. G. McKay, "Bistable surface anchoring and hysteresis of pitch jumps in a planar cholesteric liquid crystal," Eur Phys J E Soft Matter **35**(8), 74–83 (2012).

#253234 Received 4 Nov 2015; revised 30 Nov 2015; accepted 30 Nov 2015; published 3 Dec 2015

1. Introduction

The cholesteric liquid crystals (CLCs) media, possessing a unique supramolecular helical structure, has become a subject of great scientific attention for beyond-display applications, such as mirrorless band-edge lasers [1], hyper-reflectors [2], optical sensors [3], light modulators [4], and so on [5–10]. Recently, interest in CLC diffractive gratings in a fingerprint texture has emerged for nonmechanical beam steering devices [5–8], lithography masks [9] and brightness enhancement elements [10]. By virtue of the self-assembly and stimuli-responsive abilities, the easy fabrication of the CLC fingerprint texture are usually enabled by simply applying proper external electric field to aligned glass cell filled with CLCs in planar cholesteric texture [11–14]. Helfrich-Hurault instability is known to be dedicated to the formation of these undulation structures [15, 16]. Several different ways have been suggested for endowing the CLC gratings with continuous rotation ability. Most of these strategies involve either the use of a photoactive compound (nonchiral azo-dyes or chiral-photochromic dopants) in nematic LCs, an approach which produces the possibility of the reversible helical inversion by photo-illumination [17–22], or the use of different aligning conditions including hybrid-alignment [23] and photo-alignment [24]. In addition, it is recognized that two types of fingerprints can be classified according to the forming process: developable-modulation (DM) and growing-modulation (GM). The grating vector direction is dependent on the cell thickness to pitch length ratios (d/P) [7] and can be also switched between two rigorously orthogonal directions [8].

The possibility of stabilizing CLC fingerprint textures by a low-concentration polymer networks was explored as well [25–29]. The mesogenic monomers dissolved in CLCs are photo-polymerized in the fingerprint state. These networks provide anchoring capabilities which maintain the liquid crystalline order in bulk and do not seriously interrupt the morphology of the CLC system. These polymer-stabilized CLC gratings (PSCLCs) can operate in the absence of an applied electric field and exhibit a millisecond-scale response to low voltage in either the Bragg or Raman-Nath limits. Efforts have been made to understand the effect of monomer mesogenicity on the morphology of polymer network [26], director configuration of the host liquid crystal [27], variations in the diffraction properties and the optimization of the performance of electrooptical properties [28, 29]. However, to the best of our knowledge, DM and GM type polymer stabilized CLC gratings were not actually distinguished on purpose and it is not yet reported that the coexistence of both types of CLC fingerprint textures can be contemporaneously stabilized and be simultaneously patterned. Furthermore, the DM and GM gratings in glass cells with consistent alignment conditions would result in diffractions in orthogonal directions with polarization-dependent properties. Specific techniques for multi-domain alignments, like photo-alignment and micro-rubbing, etc., is not required in this process. These in-plane CLC helical superstructures would lead to a higher level of complexity and open up a new door to the design of novel advanced photonic devices.

Herein, we demonstrates that stabilized CLC gratings with interlaced DM/GM fingerprint textures are facilely achieved by varying the applied voltage and sequentially photopolymerizing the mesogenic monomers dissolved in the liquid crystal host through photomasks with stripe and checker patterns. The precedence orders of UV exposure procedure are of vital importance. The orientation of the grating stripes and the uniformity of morphologies are characterized and compared under crossed polarizing optical microscopy (POM) and scanning electron microscopy (SEM). The optimized results suggest that the polymerization of DM type fingerprint texture should be prior to that of GM texture to preserve the structural integrity. These distinct interlaced helical superstructures were based on polymer stabilized CLCs and the polarization-dependent properties were also investigated by the diffraction measurements.

#253234 Received 4 Nov 2015; revised 30 Nov 2015; accepted 30 Nov 2015; published 3 Dec 2015

2. Experimental

In the experiment, the sample was prepared with a mixture of nematic liquid crystal E7 (Xianhua, China) (positive dielectric anisotropy $\Delta\varepsilon = 13.9$ at $f = 1$ kHz, refractive indices $n_o = 1.5330$, $n_e = 1.7510$ at 20°C, elastic constants $K_{11} = 11.7 \times 10^{-12}$ N, $K_{22} = 8.8 \times 10^{-12}$ N, $K_{33} = 19.5 \times 10^{-12}$ N), reactive mesogenic monomer RM257 (1,4-bis[3-(acryloyloxy)propyloxy]-2-methyl benzene, Sdyano, China), chiral dopant S811 (Xianhua, China), and photoinitiator Irgacure 651 (2,2-dimethoxy-2-phenyl acetophenone, Ciba). The PSCLC mixture contains E7, RM257, S811 and Iragcure 651 with concentration 90.5 wt%, 7 wt%, 2.5 wt% and 1 wt%, respectively. The S811 has a helical twisting power (HTP) value of $1/(PC) = -10.9$ μm^{-1} [30], where C is the doped S811 weight percentage and P is the natural pitch. So the CLC that we yield here has a calculated pitch length of $P = 3.58$ μm by assuming that the replacement of partial E7 by RM257 with the same weight doesn't influence the HTP value for S811 in the nematic host. After homogeneous mixing, an empty cell was made from two indium-tin-oxide (ITO) glass plates coated with antiparallel-rubbed polyimide layers and filled with the mixture. Herein, the thickness of the cell was $d = 5.2 \pm 0.1$ μm, the cell gap to natural pitch length ratio of the sample is $d/P = 1.45$.

In order to prepare the interlaced patterns and determine how fine the photo-polymerization process could be, we used a collimated and unpolarized UV light source (Omnicure S2000, 365 nm, 20 mW/cm^2) through two types of photomasks with stripe and checker patterns, respectively. Here, the period of the photomask with stripe patterns is 200 μm and the period of the photomask with checker patterns is 300 μm. The size of exposed patterns is reduced to half of the corresponding photomasks by projecting UV light on the sample using a 2X objective lens. The duration time of each UV procedure is 6 s, thus making a total UV exposure duration of 12 s. Three exposure sequences were schematically illustrated in Fig. 1. **Sequence 1** can be described in this order: Initially, the photomask is inserted in the exposure light path and the 1st UV polymerization *with photomask* is performed when GM type CLC gratings exist under a consistent voltage of 4.7 V. Then the photomask is removed and the 2nd UV polymerization *without photomask* is carried out in the DM grating state (3.6 V) after it has gone through a homeotropic state (10.3 V). Similarly, in **Sequence 2**, after implementing the patterned GM gratings by 1st UV polymerization *with photomask*, we obtain the transient planar texture (1.2 V) by dropping the voltage from the homeotropic state (10.3 V) and regenerate the DM grating state for the second time (3.6 V). On this basis, the DM type CLC gratings experience the 2nd UV polymerization *without photomask* and are stabilized while the photomask is removed. As we mentioned above, more perfect DM type gratings can be prepared from transient planar state in a way by emerging all over the cell. Furthermore, we changed the exposure order of DM and GM gratings in **Sequence 3** to see the difference. Here, the DM type CLC gratings were firstly patterned by the 1st UV polymerization *with photomask* when they are generated from transient planar state. When the applied voltage is turned off, the sample returns back to the planar state. Subsequently, the GM gratings are 2nd UV-polymerized *without photomask* in the second voltage-applying round.

To further characterize the polymer network in the patterned region by scanning electron microscopy (SEM), the cell is immersed in a hexane/dichloromethane co-solvent (70/30 v/v) at room temperature for several days to evacuate the unpolymerized liquid crystals. Then the substrates are carefully disassembled with little disturbance of the structure of the polymer network.

A crossed POM (Nikon 50i) was used to observe dynamic change of the pristine sample before photo-polymerization with different voltages (peak-to-peak value, AC square wave, 1 kHz). The surface morphology of the polymer network in the disassembled cell is characterized by SEM (Hitachi S4800). A linearly polarized He-Ne laser ($\lambda = 633$ nm) is used as a probe beam. A rotatable half-waveplate is placed between the He-Ne laser and the

#253234 Received 4 Nov 2015; revised 30 Nov 2015; accepted 30 Nov 2015; published 3 Dec 2015

sample to control the incident polarization. The diffraction patterns are captured by a digital camera (Canon EOS, 600D). To investigate the dependence of diffraction intensity on polarization state and applied voltage, a silicon detector (Thorlabs PDA36A), a programmable function signal generator/oscilloscope (Hantek 3064A) and an AC voltage amplifier are used to monitor the intensity of different diffraction orders.

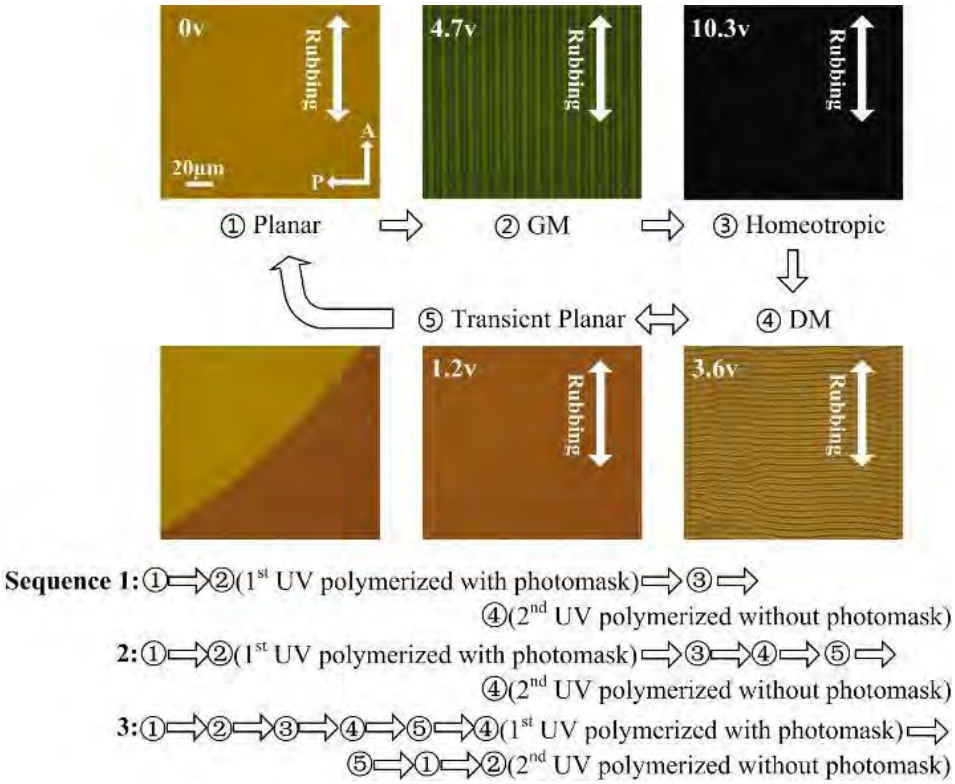

Fig. 1. Electrically switching textures of CLC mixture observed under a POM; the corresponding steps of three experimental methods illustrated. White arrows denote the polarizer and analyzer transmission axes respectively. Double-headed arrow denotes the rubbing direction.

3. Results and discussion

As shown in Fig. 1, the planar cholesteric texture was obtained by naturally cooling down the sample from clear point without applied voltage. The LC molecules are twisted from bottom to up and the axis is standing to the substrates. When the applied voltage was slightly increased to 4.7 V, the GM type fingerprint texture was obtained with its stripe direction parallel to the rubbing direction. The GM type grating stripes nucleate near edges and defects and slowly extend to the whole cell. When the voltage exceeded 10.3 V, the LC molecules were aligned vertically and a uniform dark state, namely homeotropic texture, was observed. Then the voltage was decreased to 3.6 V, the DM type fingerprint texture appeared with stripe direction perpendicular to the rubbing direction. The DM type grating emerges all over the cell in the moment in a way similar to the development of photographic image. Here, we continued to further decrease the voltage to 1.2 V, the CLC transient planar texture was observed. In particular, the transient planar texture is a meta-stable texture with the effective pitch $P^* = (K_{33}/K_{22})P$ [8, 31]. Here, the P^* is 2 times higher than P and the d/P^* is about 0.65. The direction of cholesteric grating vectors is determined by the director direction of CLC molecules in the middle layer, which is mutually perpendicular between the planar and

#253234 Received 4 Nov 2015; revised 30 Nov 2015; accepted 30 Nov 2015; published 3 Dec 2015

the transition planar zone [8, 31]. The analysis can interpret why the direction of DM/GM type grating stripes is orthogonal. Notably, if we abruptly increased the applied voltage to 3.6 V at this stage, a DM type grating appeared again. Finally, the electric field was turned off, the CLC sample transited to transient planar texture firstly and returned to the planar texture in a few minutes. As is seen, both GM and DM type gratings can be observed successively in the same sample with a suitable *d*/*P* value (1.45) on this occasion with the addition of RM257. This process is completely reversible and it is promising to achieve the stabilization of the designated texture by sustaining a proper voltage and carrying out the sequential UV-induced polymerization.

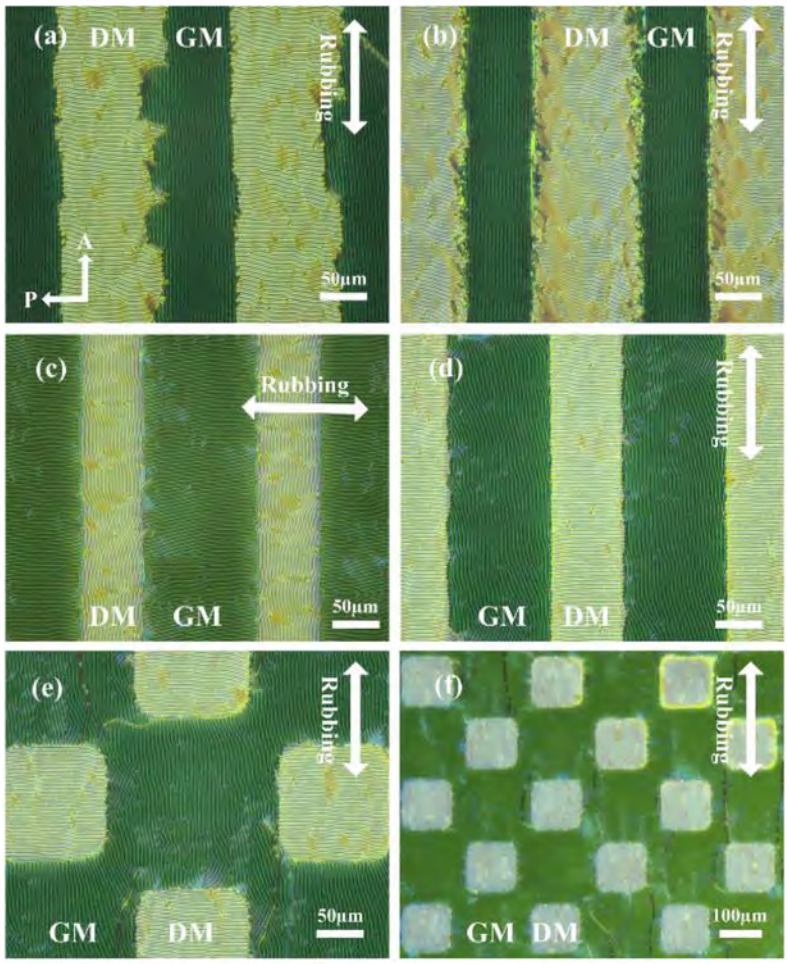

Fig. 2. POM images of stripe-patterned and checker-patterned structures based on PSCLC gratings fabricated by via (a) Sequence 1, (b) Sequence 2, and (c-f) Sequence 3. White arrows denote the polarizer and analyzer transmission axes respectively. Double-headed arrow denotes the rubbing direction.

Figure 2 displays the interlaced fingerprint textures with stripe and checker-type domains obtained following the above described exposure sequences, where the direction of DM/GM type PSCLC grating stripes is orthogonal. The periods for the DM and GM type gratings are measured to be ~4.5 μm and ~3.9 μm, respectively. In Figs. 2(a) and 2(b), the boundaries of the patterned stripes are not clear and the GM and DM gratings are even interwoven if the GM gratings are firstly polymerized. Considering the relationship between the general directions of the patterned stripes and the vectors of GM and DM gratings, two orthogonal

#253234 Received 4 Nov 2015; revised 30 Nov 2015; accepted 30 Nov 2015; published 3 Dec 2015

cases can be classified and proposed by rotating the stripe-patterned photomask before 1st UV polymerization. Especially, only if the direction of the GM gratings vector is perpendicular to the direction of patterned stripes, it is possible to implement the DM type gratings via **Sequence 1 and 2**. Otherwise, the stripes of the GM gratings are almost interconnected between adjacent patterned stripes and occupied the domains that are supposed to be filled with DM gratings when the whole exposure procedure is completely executed. Besides, the efforts, involving the variation of UV exposing duration and the stripe period of the photomask, are inoperative. It is already known that the growth of GM type gratings is a voltage-dependent step-wise process [32–37]. More and more GM grating stripes are generated and will progressively penetrate into the DM grating domain while the voltage is decreased from 10.3 V to 3.6 V. But this scene is not observed in the pristine sample before photo-polymerization. We suspect that the polymer network formed at the boundaries of GM stripes serves as defects that facilitate the nucleation of GM gratings, which grow slowly and extend into the unexposed domain when the voltage is further varied to achieve the DM grating state.

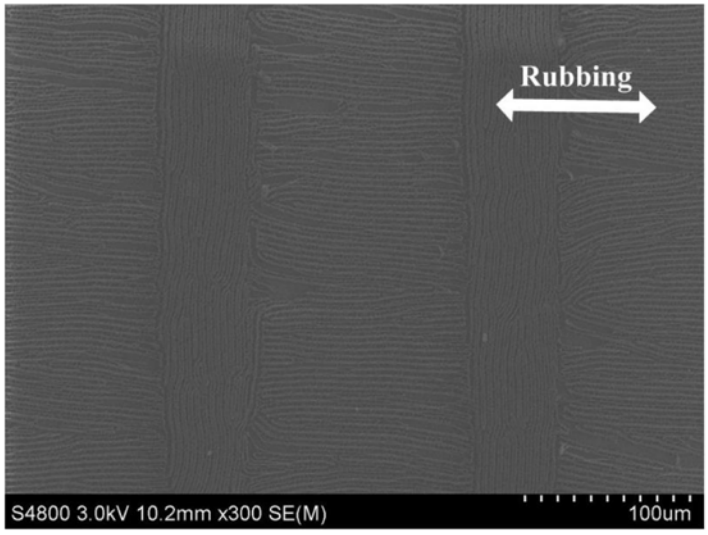

Fig. 3. SEM image of the stripe-patterned PSCLC gratings corresponding to Fig. 2(c). Double-headed arrow denotes the rubbing direction.

Surprisingly, as presented in Figs. 2(c) and 2(d), it is well-marked that not only the boundaries but also the periodicity of the alternative patterned domains are all uniform and distinct when we polymerize the DM gratings firstly via **Sequence 3**. Given that d/P^* ratio is about 0.65, it is reasonable to obtain more uniform DM fingerprints when increasing the voltage from the transient state. The vector direction of GM gratings can be fabricated either parallel or perpendicular to the patterned stripes by simply rotating the same photomask with stripe patterns in the 1st UV polymerization. The growth of GM gratings can only occur in restricted unexposed domains. The defects created at the boundaries were interconnected by GM grating stripes. As illustrated in Fig. 3, this point can be confirmed by the SEM characterization of the surface morphology of the disassembled cell with stripe-patterned PSCLC gratings, which is corresponding to Fig. 2(c). The irregular and distortion problems are solved in this manner although the GM gratings are still disturbed by some remaining oily streaks. Besides, interlaced DM/GM grating structures with checker patterns can be prepared as shown in Figs. 2(e) and 2(f). It can be anticipated that much more complex and perfect in-plane helical CLC superstructure with DM/GM fingerprint gratings can be realized by

#253234 Received 4 Nov 2015; revised 30 Nov 2015; accepted 30 Nov 2015; published 3 Dec 2015

integrating this specific feature with the recent advance of Digital Mirror Device (DMD) based photo-alignment techniques [24].

Figures 4(a)-4(d) illustrate diffraction patterns of the two types of interlaced stripe-patterned DM/GM gratings corresponding to Figs. 2(c) and 2(d), respectively. It is ascertained that the GM gratings give rise to the major diffraction in the vertical direction in Figs. 4(a) and 4(b) and the horizontal direction in Figs. 4(c) and 4(d). The other major diffractions in the orthogonal direction can be attributed to DM gratings. In Figs. 4(a) and 4(c), the polarization state of the probe beam is perpendicular to the direction of the GM grating vector, that is, parallel to the DM grating vector. In Figs. 4(b) and 4(d), the polarization of probe beam is parallel to the GM grating vector. The insets depict the fine detail of 0th order major diffraction spot, which can be verified by the simulation of spatial frequency spectrum using the well-known scalar diffraction theory. It should be addressed that the small-spacing minor diffraction spots in the major 0th order diffraction are contributed by the long-period DM/GM stripes. Our theoretical analysis also indicates that higher order major diffraction patterns should have similar fine details as 0th order pattern does. But no fine detail was detected for ± 1/2 and ± 1st orders diffraction patterns in our study. This may be due to the deformation of GM and DM gratings which is characterized by the arc-shaped patterns of diffraction spots belonging to ± 1/2 and ± 1st orders, instead of circular-shaped spots that one expects. We believe that there is still a lot to improve the shape of nonzero major diffraction spot pattern and find out the minor diffraction details.

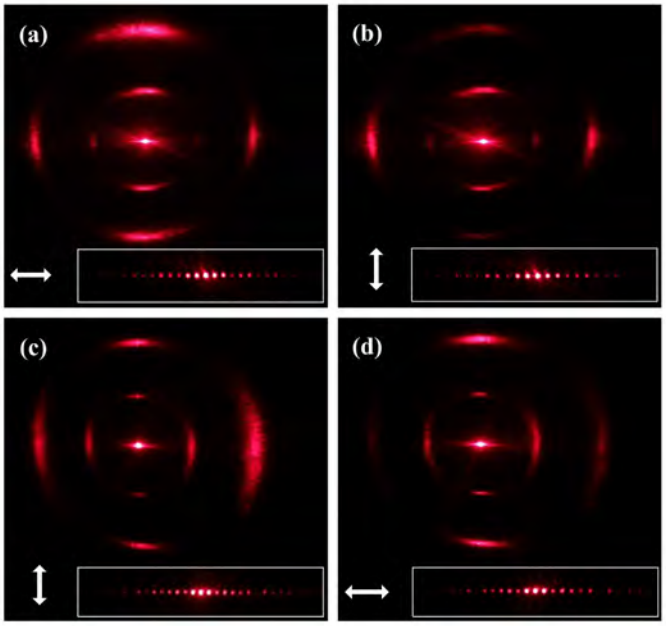

Fig. 4. Diffraction patterns of PSCLC gratings from stripe-patterned gratings shown in Fig. 2(c) and 2(d). The double-headed arrow represents the polarization state of the probe beam, which is perpendicular (a, c) and parallel (b, d) to GM grating vector. The insets plot the minor diffraction patterns in 0th order major diffraction spot. The distance from sample to the viewing screen is 25 cm. The distances between 0th order and ± 1/2, ± 1st orders of GM gratings are 4.1 cm and 8.7 cm, respectively; the distances between 0th order and ± 1/2, ± 1st orders of DM gratings are 3.6 cm and 7.4 cm, respectively.

Restated, the vectors of DM and GM gratings are orthogonal in the interlaced structures. So, the nonzero order diffraction efficiency is the highest if the polarization of the probe beam is perpendicular to the grating vector. Meanwhile, the diffraction efficiency in the orthogonal direction would be the lowest. This phenomenon can be intuitionally observed in Fig. 4 and is

#253234 Received 4 Nov 2015; revised 30 Nov 2015; accepted 30 Nov 2015; published 3 Dec 2015

then quantified by measuring the dependence of diffraction efficiencies on incident beam polarized angles with respect to the GM grating vector. The polarized angle is defined to be zero when the polarization state of the probe beam is perpendicular to the direction of the GM grating vector. As shown in Fig. 5(a), the diffraction intensity of 1/2 and 1st orders of GM and DM grating changes inversely while rotating the polarization of the probe laser beam. This polarization-dependent property provides an interesting mechanism for light redistribution in the orthogonal directions. The ratio of 1st order diffraction intensities of GM grating to DM grating is calculated and plots in the inset of Fig. 5(a), ranging from ~0.2 to ~1.8. In addition, as indicated in Fig. 5(b), the variation of zero order diffraction is non-ignorable. By assuming an ideal in-plane helical DM/GM structures, it is understandable that the nonzero diffraction would vanish when a suitable linear polarization state is chosen. For example, when a beam polarized perpendicular to GM grating vector, the light "sees" an ordinary index of refraction throughout the DM grating and a GM grating with a maximum index modulation than that seen by light polarized at other angles. Ideally, it should result in no diffraction in orthogonal direction attributed to DM grating when the highest diffraction in the GM direction is achieved and vice versa. However, it is experimentally revealed that these DM and GM diffractions always exist. A proper explanation is that the linearly polarized incident light becomes elliptically polarized with its major axis rotates with LC directors in the sample when the Mauguin's limit is not fully satisfied with a d/P~1.45 [7].

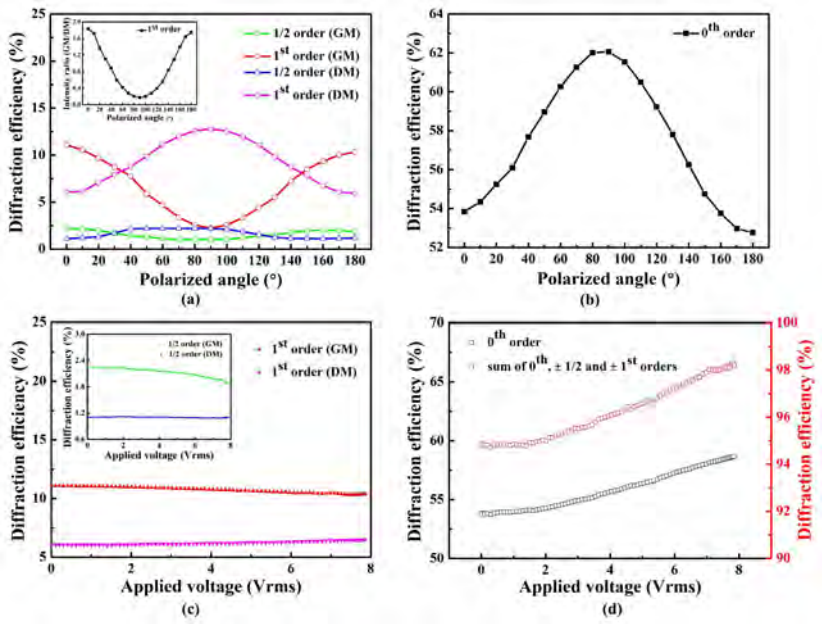

Fig. 5. The diffraction properties of stripe-patterned PSCLC gratings shown in Fig. 2(d). (a) The dependence of diffraction efficiency of 1/2 and 1st orders of GM and DM gratings on polarized angle. The polarized angle is defined to be relative to the GM grating vector. The inset plots the intensity ratios of 1st order diffraction intensities contributed by GM and DM gratings. (b) The dependence of 0th order diffraction efficiency on polarized angle. (c) The dependence of diffraction efficiency of 1st order of GM and DM gratings on applied voltage. The inset shows the dependence of diffraction efficiency of 1/2 order of GM and DM gratings on applied voltage. (d) The dependence of 0th order and sum of 0th, ± 1/2 and ± 1st orders of GM and DM gratings diffraction efficiency on applied voltage.

Figure 5(c) shows the relationship between the applied voltage and nonzero order (± 1/2 and ± 1st orders) major diffraction efficiency of both GM and DM gratings. And Fig. 5(d) shows the dependence of 0th order and sum of 0th, ± 1/2 and ± 1st orders of GM and DM gratings diffraction efficiency on applied voltage. In all cases, the polarization state of the

#253234 Received 4 Nov 2015; revised 30 Nov 2015; accepted 30 Nov 2015; published 3 Dec 2015

probe beam is fixed to be perpendicular to the GM grating vector. Although the CLC gratings are supposed to be firmly stabilized by the UV-induced polymerization of mesogenic monomers, the diffraction behavior can still be slightly tuned by external electric field. It is notable that the diffraction intensity of DM grating is pretty stable and that of GM grating is more vulnerable. This intriguing tunable capability provides a useful complement to tune the light redistribution in the orthogonal directions.

4. Conclusions

In conclusion, we demonstrate a flexible method to stabilize different types of interlaced DM/GM fingerprint textures in the same cell by means of sequential photopolymerization of CLCs doped with reactive mesogenic monomer. Intriguing stripe-patterned and checker-patterned in-plane helical superstructures are prepared via three different exposure sequences and the morphologies were investigated under POM and SEM. It is crucial that DM gratings should be stabilized before GM gratings to achieve uniform patterns with well boundaries. Furthermore, polarization-dependent diffraction measurements are coincident with observed PSCLC structures and we also reveal the mechanism for redistribution of nonzero diffraction intensity in orthogonal directions by changing the polarization state of incident laser beam and applying external electric field. In the present scenario of the exploration of in-plane helical CLC superstructures, we believe that much more photonic potentials can be anticipated on account of further developments of cost-efficient and complex diffraction elements and devices based on CLC fingerprint textures.

Acknowledgments

This work was sponsored by the Fundamental Research Funds for the Central Universities (No. 20720140518), the National Natural Science Foundation of China (NSFC) (No. 61505173), the Open Foundation Project of National Laboratory of Solid State Microstructures (M28007) and the Open Foundation Project of the State Key Lab of Silicon Materials (No. SKL2015-02). The authors like to thank Prof. Han-Ying Li and Dr. Tao Ye of Zhejiang University for the SEM measurements.

#253234 Received 4 Nov 2015; revised 30 Nov 2015; accepted 30 Nov 2015; published 3 Dec 2015